Published for SISSA by Springer

Received: April 25, 2022
Revised: September 16, 2022
Accepted: September 28, 2022
Published: October 7, 2022

Electroweak phase transition in 2HDM under Higgs, Z-pole, and W precision measurements

Huayang Song,[c,1] **Wei Su**[a,b,2] **and Mengchao Zhang**[d,1]

[a] *School of Science, Shenzhen Campus of Sun Yat-sen University, No. 66, Gongchang Road, Guangming District, Shenzhen, Guangdong 518107, P.R. China*

[b] *Korea Institute for Advanced Study, Seoul 02455, Korea*

[c] *CAS Key Laboratory of Theoretical Physics, Institute of Theoretical Physics, Chinese Academy of Sciences, Beijing 100190, P.R.China*

[d] *Department of Physics and Siyuan Laboratory, Jinan University, Guangzhou 510632, P.R. China*

E-mail: huayangs@itp.ac.cn, suwei26@mail.sysu.edu.cn, mczhang@jnu.edu.cn

Abstract: In this work we revisit the existence of a strong first order electroweak phase transition (SFOEWPT) and recent m_W precision measurement in the Type-I and Type-II 2HDMs. The $\mathcal{O}(100)$ GeV new scalars in 2HDMs are favored by SFOEWPT, which is necessary for electroweak baryogenesis, and observed m_W shift as well. We find that under current constraints, both Type-I and Type-II 2HDM can explain the SFOEWPT, Z-pole, Higgs precision measurements and m_W precision measurement of CDF-II at same time, and all these precision measurements are sensitive to heavy Higgs mass splitting in 2HDM. The allowed regions are $\Delta m_{A/C} \in (-400, 400)$ GeV, $\tan\beta \in (1, 50)$, and $\Delta m_{A/C} \in (-200, 300)$ GeV, $\tan\beta \in (1, 10)$ for Type-I and Type-II 2HDM respectively. Furthermore future lepton collider measurements on Higgs and Z boson properties can explore this scenario in more detail or even rule out it.

Keywords: Multi-Higgs Models, Electroweak Precision Physics

ArXiv ePrint: 2204.05085

[1] First author.
[2] Corresponding author.

https://doi.org/10.1007/JHEP10(2022)048

JHEP10(2022)048

Contents

JHEP10(2022)048

1 Introduction

With the discovery of the Higgs boson at the Large Hadron Collider (LHC) in 2012 [1, 2], particle physics has been entering a new era. Due to the lack of direct search result at LHC, precision studies of particle physics are becoming important. The current measurements of particle properties seem to be consistent with all other categories of experiments and can be described by the Standard Model (SM) quite well. Meanwhile there are compelling arguments, both from theoretical and observational viewpoints, in favor of new physics beyond the Standard Model (BSM). The CDF collaboration has recently reported a precise measurement of the W boson mass, which indicates a significant tension with the previous measurements and the SM prediction [3]. Although this result needs to be further confirmed by other experiments, such as D0, ATLAS, and CMS, it is still an exciting possible signal indicating the existence of new physics at a place not far above the electroweak (EW) scale.[1]

Given this possible signal, the following question is which new physics does this possible signal point to. Among different kinds of BSM new physics, electroweak baryogenesis (EWBG) [12, 13] is likely to be relevant to the current possible signal. EWBG was proposed

[1] Recent study on the new CDF result see [4–11].

to explain the observed baryon asymmetry of the universe (BAU). Through the baryon number breaking sphaleron process [14–16] and CP violating scattering with bubble wall, net baryon number can be produced during the nucleation process of Higgs field. To trigger the nucleation process and to prevent the generated net baryon being washed out, the electroweak phase transition (EWPT) needs to be a strong first order phase transition. However, due to current measured Higgs mass, the SM EWPT is not even first order [17, 18].

Therefore new particles are definitely required for a strong first order electroweak phase transition (SFOEWPT). Furthermore, new particles that help to trigger SFOEWPT can not be too heavy compared to the EW scale, otherwise they will be decoupled in the thermal phase transition process and lose effect. Thus, the new measurement of the W boson mass might be a hint of EWBG.

One method to trigger SFOEWPT is augmenting the SM Higgs sector by additional scalars, and it has been studied intensively in the literature [19–41]. Extending the Higgs sector by a singlet scalar seems to be the simplest choice, but it is difficult for such model to explain the observed m_W under current limits [42]. In this work we choose Two-Higgs-Doublet Models (2HDMs) [43, 44], which extend the SM Higgs sector by another doublet, as the benchmark model to study the relationship between SFOEWPT and m_W. After electroweak symmetry breaking, in addition to the SM-like Higgs boson h, there are three non-SM Higgs bosons, $H/A/H^{\pm}$, which can have masses below TeV and couple to the SM-like Higgs h to build an energy barrier between the symmetric and broken phase. Therefore the EW phase transition can be first order and strong enough for the baryogenesis [27]. Furthermore, these light extra scalar can induce a positive m_W shift [45] and modify the predictions on the Z-pole observables like the oblique parameters S, T and U via one-loop contributions to the W and Z self-energies. The mixing between neutral scalars and extra loop corrections further modify the Higgs couplings $\kappa_i = g_{hii}^{\rm 2HDM}/g_{hii}^{\rm SM}$ relative to their SM expectations. Though the LHC measurements still give a large amount of available phase space of the 2HDM, future Higgs factories, e.g. ILC [46], FCC-ee [47, 48] and CEPC [49, 50] can measure them with unprecedented precision to further constrain the model.

In this paper, we study the constraints from precision measurements (especially the new W boson mass and future Higgs coupling measurements) on the 2HDM and explore the possible parameter space which could lead to a SFOEWPT. Our study shows that SFOEWPT is consistent with the new uplifted m_W in a certain parameter space. But due to the close connection between m_W and other precise measurements, the "SFOEWPT + m_W" scenario is in slight tension with current limits. Furthermore, the future precision lepton collider measurements of both Higgs and Z boson properties could fully rule out the allowed parameters to fulfil SFOEWPT and m_W, provided the measured central values locate in the SM prediction. Conversely, if the "SFOEWPT + m_W" scenario in 2HDM is true, than a clear deviation from SM prediction will be observed at future lepton colliders.

The rest of the paper is organized as follows. In section 2 we briefly introduce 2HDM models and related constraints. Description on EWPT is also given in section 2. In section 3 we perform a parameter space scan on a wide range and present allowed points, with future precise measurements included. We conclude this work in section 4.

JHEP10(2022)048

2 2HDM

2.1 A review

In this section, we provide a brief review of the aspects of 2HDMs. For pedagogical introduction, see ref. [44] and a recent review ref. [51] in light of current experiments. The scalar sector of 2HDMs consists two $\mathrm{SU}(2)_L$ doublets Φ_i, $i = 1, 2$, which can be parameterized as below,

$$\Phi_i = \begin{pmatrix} \phi_i^+ \\ (v_i + \phi_i^0 + iG_i)/\sqrt{2} \end{pmatrix} \tag{2.1}$$

where v_1 and v_2 are the vacuum expectation values (VEVs) of the neutral components, satisfying the relation $v \equiv \sqrt{v_1^2 + v_2^2} = 246$ GeV. Assuming CP-conservation and only a soft breaking of a discrete $\mathcal{Z}_2$ symmetry allowed, the most general Higgs potential can be expressed as,

$$\begin{aligned} V^0(\Phi_1, \Phi_2) = {} & m_{11}^2 \Phi_1^\dagger \Phi_1 + m_{22}^2 \Phi_2^\dagger \Phi_2 - m_{12}^2 \left(\Phi_1^\dagger \Phi_2 + h.c.\right) + \frac{\lambda_1}{2} \left(\Phi_1^\dagger \Phi_1\right)^2 + \frac{\lambda_2}{2} \left(\Phi_2^\dagger \Phi_2\right)^2 \\ & + \lambda_3 \left(\Phi_1^\dagger \Phi_1\right) \left(\Phi_2^\dagger \Phi_2\right) + \lambda_4 \left(\Phi_1^\dagger \Phi_2\right) \left(\Phi_2^\dagger \Phi_1\right) + \frac{\lambda_5}{2} \left[\left(\Phi_1^\dagger \Phi_2\right)^2 + h.c.\right], \end{aligned} \tag{2.2}$$

where there are eight real parameters, $\{m_{11}^2, m_{22}^2, m_{12}^2, \lambda_1, \lambda_2, \lambda_3, \lambda_4, \lambda_5\}$. After the electroweak symmetry breaking (EWSB), the scalar sector of a 2HDM consists of five mass eigenstates: a pair of neutral CP-even Higgses, h and H, a CP-odd Higgs, A, and a pair of charged Higgses $H^\pm$. We can express these states as,

$$\begin{aligned} h &= -s_\alpha\, \phi_1 + c_\alpha\, \phi_2, & A &= -\, s_\beta\, G_1 + c_\beta\, G_2, \\ H &= \;\; c_\alpha\, \phi_1 + s_\alpha\, \phi_2, & H^\pm &= -\, s_\beta\, \phi_1^\pm + c_\beta\, \phi_2^\pm, \end{aligned} \tag{2.3}$$

where we will identify h as the discovered SM-like 125 GeV Higgs.

For convenience, we will parametrize the potential of 2HDMs by the physical Higgs masses m_h, m_H, m_A and $m_{H^\pm}$, the mixing angle between the two CP-even Higgses α, $\tan\beta \equiv v_2/v_1$, the electroweak VEV v, and the soft $\mathcal{Z}_2$ symmetry breaking parameter m_{12}^2. Note that the vacuum expectation value v and the mass of the SM-like Higgs, m_h are fixed to their known values 246 GeV and 125 GeV respectively, leaving the remaining six independent parameters.

Assigning different $\mathcal{Z}_2$ parities to the SM fermions, there are four types of 2HDMs. However, in this study, we focus on the so-called Type-I and Type-II 2HDMs, where all fermions obtain their masses from a single Higgs doublet in Type-I model while up- and down-type fermions obtain their masses from differnt Higgs doublets in Type-II model. In the Type-II model the couplings between A/H and down-type fermions are enhanced by $\tan\beta$ and therefore it is usually more constrained by experiments when $\tan\beta$ is large.

2.2 Theoretical constraints on 2HDMs

The parameter spaces of 2HDMs are already constrained by theoretical consideration without experimental results.

JHEP10(2022)048

- **Vacuum stability** In order to make the vacuum stable, the scalar potential should be bounded from below [52]:

$$\lambda_1 > 0\,,\ \lambda_2 > 0\,,\ \lambda_3 > -\sqrt{\lambda_1\lambda_2}\,,\ \lambda_3+\lambda_4-|\lambda_5| > -\sqrt{\lambda_1\lambda_2} \tag{2.4}$$

- **Perturbativity and unitarity** Requiring perturbativity, we must have $|\lambda_i| \leq 4\pi$. And requiring tree-level unitarity of the scattering in the 2HDM scalar sector imposes the following additional mass constraints [53]:

$$\left|3(\lambda_1+\lambda_2) \pm \sqrt{9(\lambda_1-\lambda_2)^2+4(2\lambda_3+\lambda_4)^2}\right| < 16\pi\,, \tag{2.5}$$

$$\left|(\lambda_1+\lambda_2) \pm \sqrt{(\lambda_1-\lambda_2)^2+4\lambda_4^2}\right| < 16\pi\,, \tag{2.6}$$

$$\left|(\lambda_1+\lambda_2) \pm \sqrt{(\lambda_1-\lambda_2)^2+4\lambda_5^2}\right| < 16\pi\,, \tag{2.7}$$

$$|\lambda_3+2\lambda_4\pm 3\lambda_5| < 8\pi\,,\ |\lambda_3\pm\lambda_4| < 8\pi\,,\ |\lambda_3\pm\lambda_5| < 8\pi \tag{2.8}$$

To understand the these constraints, it is useful to consider the relations between the quartic couplings and the physical masses

$$\begin{aligned}
v^2\lambda_1 &= m_h^2 - \frac{t_\beta\left(m_{12}^2 - m_H^2 s_\beta c_\beta\right)}{c_\beta^2} + \left(m_h^2-m_H^2\right)\left[c_{\beta-\alpha}^2\left(t_\beta^2-1\right) - 2t_\beta s_{\beta-\alpha}c_{\beta-\alpha}\right],\\
v^2\lambda_2 &= m_h^2 - \frac{m_{12}^2 - m_H^2 s_\beta c_\beta}{t_\beta s_\beta^2} + \left(m_h^2-m_H^2\right)\left[c_{\beta-\alpha}^2\left(t_\beta^{-2}-1\right) + 2t_\beta^{-1} s_{\beta-\alpha}c_{\beta-\alpha}\right],\\
v^2\lambda_3 &= m_h^2 + 2m_{H^\pm}^2 - 2m_H^2 - \frac{m_{12}^2 - m_H^2 s_\beta c_\beta}{s_\beta c_\beta} - \left(m_h^2-m_H^2\right)\left[2c_{\beta-\alpha}^2 + s_{\beta-\alpha}c_{\beta-\alpha}\left(t_\beta - t_\beta^{-1}\right)\right],\\
v^2\lambda_4 &= m_A^2 - 2m_{H^\pm}^2 + m_H^2 - \frac{m_{12}^2 - m_H^2 s_\beta c_\beta}{s_\beta c_\beta},\\
v^2\lambda_5 &= m_H^2 - m_A^2 - \frac{m_{12}^2 - m_H^2 s_\beta c_\beta}{s_\beta c_\beta}.
\end{aligned} \tag{2.9}$$

We can introduce $\lambda v^2 \equiv m_H^2 - m_{12}^2/(s_\beta c_\beta)$ following ref. [54]. The above expression indicates that the unitarity and perturbativity set up upper bounds on the mass splittings, which can be roughly taken as $\lambda v^2 < 4\pi v^2$, $m_A^2 - m_H^2 \lesssim \mathcal{O}\left(4\pi v^2 - \lambda v^2\right)$, $m_{H^\pm}^2 - m_H^2 \lesssim \mathcal{O}\left(4\pi v^2 - \lambda v^2\right)$ and $\max\{t_\beta, \cot\beta\} \lesssim \sqrt{(8\pi v^2)/(3\lambda v^2)}$. Generally speaking, large mass splitting among non-SM Higgses are not allowed for large values of λv^2 and/or non-SM Higgs masses.

2.3 Direct searches at LEP and LHC

The search for pair-produced charged Higgs bosons at the Large Electron-Positron Collider (LEP) imposes a lower bound of 80 GeV on the mass of the charged Higgs boson [55], and LEP searches for AH production constrain the sum of the masses $m_H + m_A > 209$ GeV [56].

LHC are also looking for direct productions of exotic Higgses via including $A/H \to \mu\mu$ [57, 58], $A/H \to bb$ [59, 60], $A/H \to \tau\tau$ [61–63], $A/H \to \gamma\gamma$ [64–68], $A/H \to tt$ [69], $H \to ZZ$ [70, 71], $H \to WW$ [72, 73], $A \to hZ \to bb\ell\ell$ [74–77], $A \to hZ \to \tau\tau\ell\ell$ [76, 78, 79],

JHEP10(2022)048

	Current				CEPC				FCC-ee				ILC			
	σ	correlation			σ	correlation			σ	correlation			σ	correlation		
		S	T	U	(10^{-2})	S	T	U	(10^{-2})	S	T	U	(10^{-2})	S	T	U
S	0.04 ± 0.11	1	0.92	−0.68	1.82	1	0.9963	−0.9745	0.370	1	0.9898	−0.8394	2.57	1	0.9947	−0.9431
T	0.09 ± 0.14	–	1	−0.87	2.56	–	1	−0.9844	0.514	–	1	−0.8636	3.59	–	1	−0.9569
U	-0.02 ± 0.11	–	–	1	1.83	–	–	1	0.416	–	–	1	2.64	–	–	1

Table 1. Estimated S, T, and U ranges and correlation matrices ρ_{ij} from Z-pole precision measurements of the current results [88].

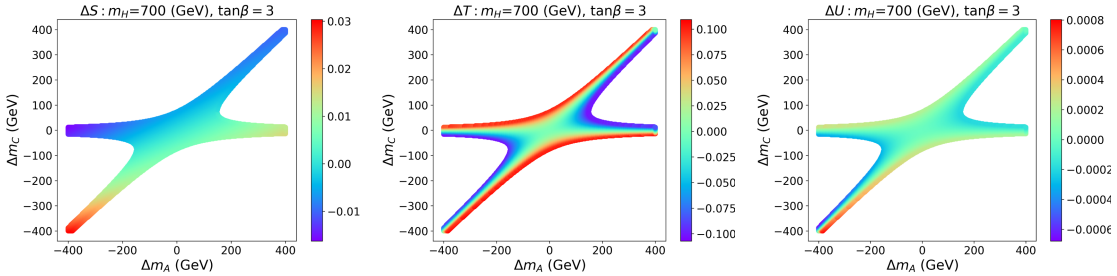

Figure 1. Current oblique constraints S, T, U in the plane of $\Delta m_A - \Delta m_C$ with $m_H = 700\,\text{GeV}$, $\tan\beta = 3$ in the alignment limit $\cos(\beta - \alpha) = 0$. The colors are for corresponding parameter value.

$H \to hh$ [80–83], and $A/H \to HZ/AZ$ [84, 85]. The null results have already ruled out a significant portion of parameter space of 2HDM. For a typical mass splitting $m_A - m_H = m_{H^\pm} - m_H = 200$ GeV , the exotic decay channel $A \to HZ$ has already excluded a neutral Higgs with mass less than $2m_t$ for $\tan\beta < 5$ in Type-I model and for $0.5 < \tan\beta < 15$ in Type-II model. For large $\tan\beta$ region ($\tan\beta > 15$) in Type-II model, this channel put the mass of neutral scalar H to be above 600 GeV. Top quarks search channels, $4t$ and $A/H \to tt$, rule out $m_H < 800$ GeV for $\tan\beta < 0.3$ and $m_H < 650$ GeV for $\tan\beta < 1.1$ in both two types of 2HDMs. While $A/H \to \tau\tau, \gamma\gamma$ can exclude the region $m < 350$ GeV, $\tan\beta < 1$ in Type-I and -II models, $A/H \to \tau\tau$ could fully exclude m_H larger than 800 GeV when $\tan\beta > 10$ in Type-II 2HDM. For a complete recasting the LHC direct search results in the 2HDM, we refer the readers to refs. [27, 51, 86].

2.4 Z-pole and Higgs precision measurements

Measurements of Z-pole observables at the Large Electron-Positron Collider (LEP) impose strong constraints on the 2HDM [87]. Satisfying Z-pole constraints requires the charged scalar mass to be close to one of the heavy neutral scalar masses: $m_{H^\pm} \simeq m_H$ or $m_{H^\pm} \simeq m_A$. In our analysis, we simply take the S, T, U data at 95% Confidence Level (C.L.) in table 1 to capture the dominant contributions from Z-pole measurements. Note that a global analysis to recast the S, T, U parameters is needed by including both Z-pole observables and latest W mass measurement [3], here for simplicity we just take them as two separate measurements and are going to discuss more on the W boson mass effects in section 2.5.

JHEP10(2022)048

To reveal the relation between non-SM Higgs spectra and S, T, U, we define following mass splitting parameters:

$$\Delta m_A = m_A - m_H, \Delta m_C = m_{H^\pm} - m_H \tag{2.10}$$

In figure 1 we present the S, T, U deviation from their SM value as functions of Δm_A and Δm_C. Constraints given in figure 1 applies to both Type-I and Type-II 2HDMs, because Yukawa couplings are irrelevant to S, T, U paramters, at least at one-loop level. The current uncertainty on the measurement of S, T, U is around 10%, so it can be seen that T parameter provides the most stringent limit on non-SM Higgs mass splitting.

The LHC has also performed high precision tests on the Higgs couplings, which indicates all the measurable couplings κ_i are close to their SM values. Future Higgs factories will further improve the precision of measurements in the Higgs sector, and we therefore include hypothetical future lepton collider results in our study after meeting the current constraints from the LHC [86, 89]. We adopt the Higgs measurements results presented in table 3 in ref. [90]. Note that for future experiments, we assume there is no deviation from the SM in Higgs measurements.

2.5 m_W in the 2HDM

An important observable used in the SM precision test is given by m_W which is closely related to Z boson mass m_Z, Fermi constant G_F, and fine structure constant $\alpha_{\rm ew}$,

$$m_W^2 \left(1 - \frac{m_W^2}{m_Z^2}\right) = \frac{\pi \alpha_{\rm ew}}{\sqrt{2} G_F}(1 + \Delta r) \tag{2.11}$$

where Δr corresponds to quantum corrections which are calculated in the 2HDM taking into account dominant $\mathcal{O}(\alpha_{\rm ew}^2)$ effects in ref. [45]. m_W correction can also be represented in terms of Peskin–Takeuchi STU parameters [91]

$$m_W^{\rm 2HDM} = m_W^{\rm SM}\left[1 + \frac{\alpha_{\rm ew} {c_W}^2}{2\left({c_W}^2 - {s_W}^2\right)} T(1 + \delta\rho^{\rm 2HDM}) + \frac{\alpha_{\rm ew}}{8 {s_W}^2} U - \frac{\alpha_{\rm ew}}{4\left({c_W}^2 - {s_W}^2\right)} S\right] \tag{2.12}$$

to the $\mathcal{O}(\alpha_{\rm ew}^2)$, where $m_W^{\rm SM} = 80.357\ {\rm GeV} \pm 4_{\rm (inputs)} \pm 4_{\rm (theory)}\ {\rm MeV}$ [3], the expressions for the oblique parameters S, T, U can be found in ref. [88], $\delta\rho^{\rm 2HDM} = \frac{|\lambda_{hhh}^{\rm 2HDM}|^2}{16\pi^2 m_h^2}$ are higher order 2HDM effects from enhanced Higgs boson self-interactions, and $\alpha_{\rm ew} = 1/127.951$ is the $\overline{\rm MS}$ fine structure constant at the scale $\mu = m_Z$ [92]. The current constraint on $\kappa_{hhh} = \lambda_{hhh}^{\rm 2HDM}/\lambda_{hhh}^{\rm SM}$ is between $(-1.0, 6.6)$ [93] so that the higher order effect $\delta\rho^{\rm 2HDM}$ up to $\mathcal{O}(0.01)$ is weak.

For covenience, we define

$$\Delta m_W^{\rm 2HDM} = m_W^{\rm 2HDM} - m_W^{\rm SM}. \tag{2.13}$$

In the left panel of figure 2 where we take $\Delta U = 0$ as a benchmark case, we show the general picture of $\Delta m_W^{\rm 2HDM}$ in the plane of $\Delta T - \Delta S$ based on the allowed region shown in the figure 1. The colors show values of $\Delta m_W^{\rm 2HDM}$, varying from -50 MeV to 50 MeV.

JHEP10(2022)048

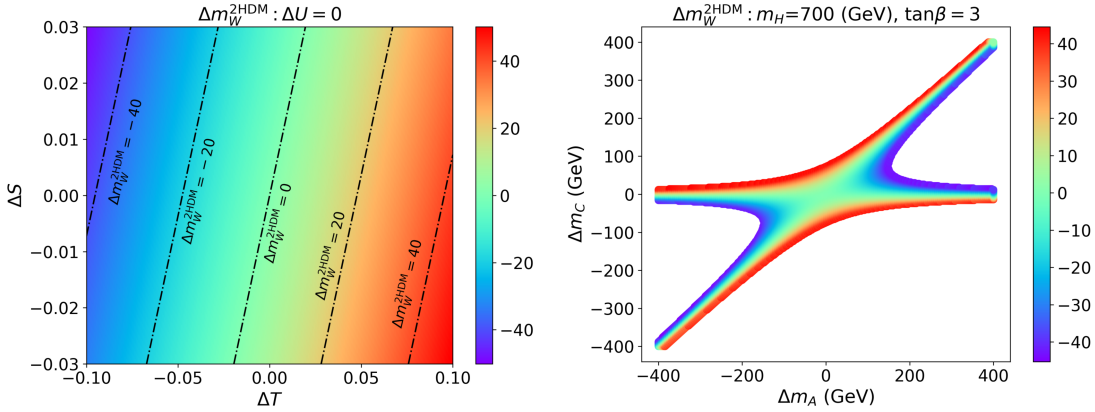

Figure 2. (Left): general picture of $\Delta m_W^{\rm 2HDM}$ in the plane of $\Delta T - \Delta S$ with $\Delta U = 0$. The colors are values of $\Delta m_W^{\rm 2HDM}$, varying from -50 MeV to 50 MeV. We have 5 black dash-dotted lines for $\Delta m_W^{\rm 2HDM} = -40, -20, 0, 20$, and 40 MeV. (Right): $m_W^{\rm 2HDM}$ in the plane of $\Delta m_A - \Delta m_C$ with same benchmark spectrum $m_H = 700$ GeV as figure 1. The colors are same to the left panel.

We have 5 black dash-dotted lines for $\Delta m_W^{\rm 2HDM} = -40, -20, 0, 20$, and 40 MeV. Generally speaking, $\Delta m_W^{\rm 2HDM}$ mainly depends on ΔT, and the larger ΔT and smaller ΔS result in large $\Delta m_W^{\rm 2HDM}$. This result can be easily understood with the signs of the coefficients in front of S, T, U in eq. (2.12). In the right panel, we take the benchmark spectrum of figure 1 with $m_H = 700$ GeV and $\tan\beta = 3$, and show $\Delta m_W^{\rm 2HDM}$ in the plane of $\Delta m_A - \Delta m_C$. We can see that, under current various constraints, the benchmark spectrum here can provide the theoretical correction matching the new experimental measurement at CDF-II [3]. In the 2HDM, $\Delta m_W^{\rm 2HDM}$ is directly related to oblique parameters, and oblique parameters further depend on non-SM Higgs mass splitting Δm_A and Δm_C. So it is clear that $\Delta m_W^{\rm 2HDM}$ is sensitive to non-SM Higgs mass splitting.

2.6 Flavor constraints

The charged Higgs $H^\pm$ boson couples to both up and down type fermions, which can lead to flavor changing processes strongly constrained by flavor physics observations. The most stringent of limits comes from the measurements of B-meson decays (e.g. $b \to s\gamma$ and $B^+ \to \tau\nu$), which disfavor $m_{H^\pm} < 800$ GeV and large values of $\tan\beta$ respectively in Type-II 2HDM [94–97], or $m_{H^\pm} < 1$ TeV and small values of $\tan\beta$ ($\tan\beta < 1$) in Type-I model [97]. However, not all experimental results in flavor physics can be alleviated within 2HDM framework [94, 98]. Therefore, given the uncertainties involved in those flavor measurements, we only give a few comments on the constraints from B-physics on the scalar sector but do not take them in this paper.

2.7 Phase transition in the 2HDM

To study EWPT, we need to know the thermal effective potential, which is the free-energy density, as the function of scalar VEVs. The thermal effective potential $V(\phi_1, \phi_2, T)$ can

JHEP10(2022)048

be schematically expressed as:

$$V(\phi_1, \phi_2, T) = V^0(\phi_1, \phi_2) + V^{\rm CW}(\phi_1, \phi_2) + V^{\rm CT}(\phi_1, \phi_2) + V^{\rm T}(\phi_1, \phi_2, T). \quad (2.14)$$

Here ϕ_i are scalar VEVs, T is the temperature of thermal system, $V^0(\phi_1, \phi_2)$ is the tree-level potential, and $V^{\rm CW}(\phi_1, \phi_2)$ is the Coleman-Weinberg potential [25]. Counter term $V^{\rm CT}(\phi_1, \phi_2)$ is added to cancel the VEVs and scalars masses shift caused by $V^{\rm CW}(\phi_1, \phi_2)$ [39]. Thus our input parameters, i.e. masses and mixing angles, can be considered as physical parameters. $V^{\rm T}(\phi_1, \phi_2, T)$ is thermal correction with daisy graphs re-summed [26].

In the very early universe, temperature T is much higher than all the particles' masses in our model. The large effective thermal mass keeps ϕ_i at zero and thus maintain the EW-symmetry. And when T become much lower than EW scale, the global minimum position of $V(\phi_1, \phi_2, T)$ on $\phi_1 - \phi_2$ plane must move to a place where $\phi_1^2 + \phi_2^2 \neq 0$ to break EW-symmetry. To know whether this phase transition process is first-order, we can track the minimum point with T decreasing. If the minimum point (which locates in zero point when T is very large) "jump to" a non-zero point discontinuously at critical temperature T_c, then the EWPT should be first-order. This method has been numerically implemented in public package `BSMPT` [99]. We will use this package in this work.

Furthermore, to prevent baryon number being washed out inside Higgs bubble, the "wash out" parameter [24] $\xi_c \equiv v_c/T_c$ (v_c is the Higgs VEV at T_c) should roughly be larger than 1. Considering the uncertainty in ξ_c calculation [28, 29, 35–38], we use a slightly looser criteria for SFOEWPT:

$$\xi_c \equiv \frac{v_c}{T_c} > 0.9. \quad (2.15)$$

3 Study results

In this section, we try to explore the SFOEWPT under various current and future constraints. Specially we have a detailed study about the latest m_W result at CDF-II.

We will firstly have a large amount of random scan points, and our study include the theoretical constraints, B-physics, LHC Run-II direct searches, current precision measurement of Higgs and Z-pole physics. Then the further study is performed at future Higgs factories, including CEPC, FCC-ee and ILC as shown in table 1, to confront the SFOEWPT and m_W anomaly. Our theoretical calculation of SM-like Higgs precision measurements[2] works at one-loop level, involving its productions and decays.

3.1 Study method

We perform a 6 parameters random scan for both Type-I and Type-II, and the scan regions are:

$$\tan\beta \in (0.2, 50), |\cos(\beta - \alpha)| < 0.5\,, \quad m_{A/H^\pm} \in (10, 1500)\ \text{GeV}\,,$$
$$m_{12}^2 \in (0, 1500^2)\ \text{GeV}^2, \qquad m_H \in (130, 1500)\ \text{GeV}.$$

[2]Here and later we will have "Higgs precision measurements" for the theoretical calculation of SM-like Higgs measurements. In this work, they are calculated at one-loop level.

JHEP10(2022)048

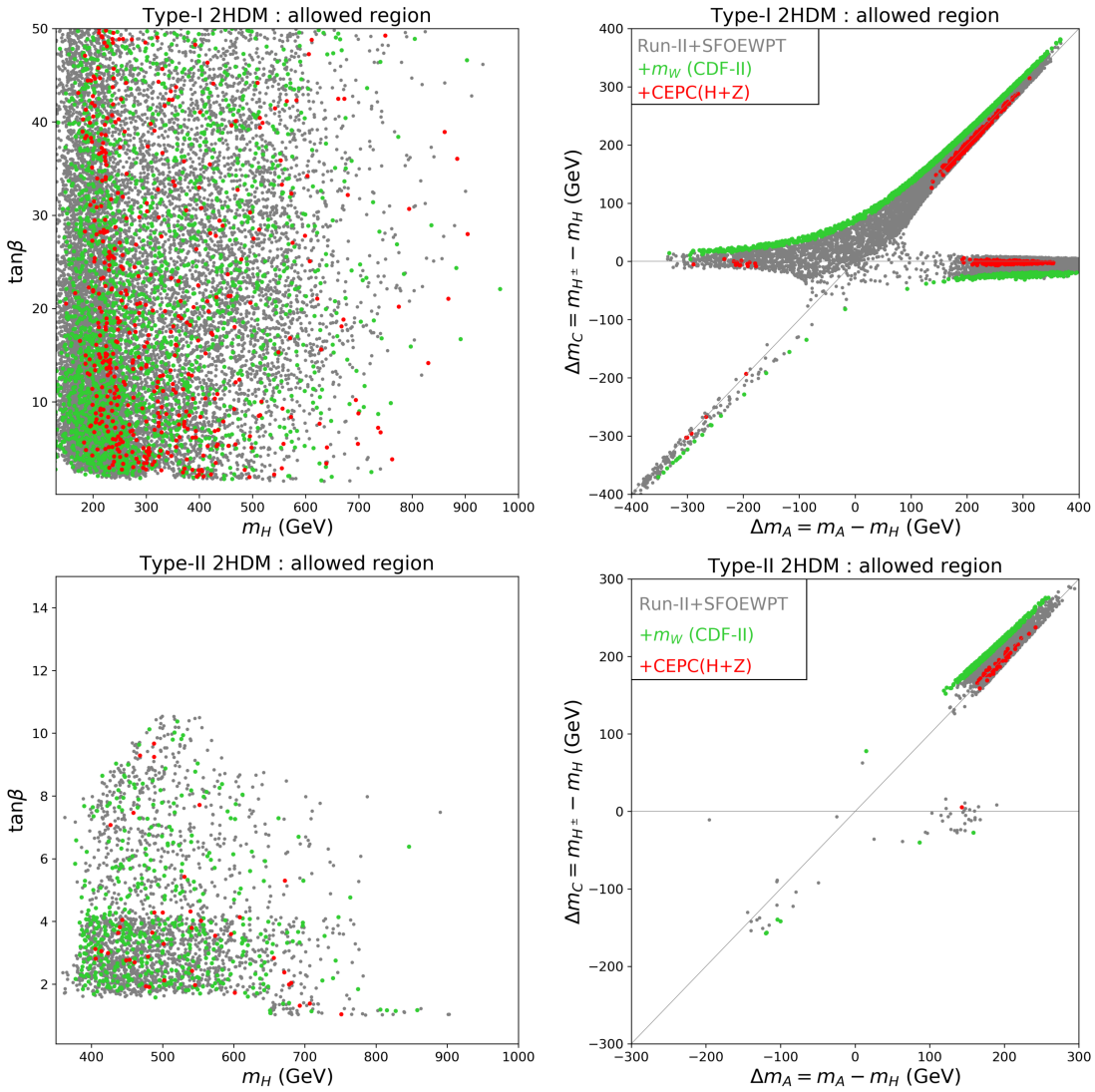

Figure 3. The allowed parameter space in the plane of $m_H - \tan\beta$ (left), $\Delta m_A - \Delta m_C$ (right). The grey points survive all theoretical constraints, current experimental constraints, and the conditions of SFOEWPT. The top and bottom panels are for Type-I and Type-II respectively. The green ones are able to provide a m_W by CDF-II, while the red ones are allowed by future Higgs and Z-pole precision measurements from CEPC. The red and green points do not cover each other.

The number of samples allowed by the various applied theoretical and experimental constraints (except for m_W from CDF-II) is more than 1 million (of 1 billion points in total) . After considering the SFOEWPT, it is about a few hundreds of thousands points allowed for Type-I, but much less for Type-II to be shown in figure 3 as grey dots.

To incorporate in the m_W at CDF-II, here in the 2HDM based on eq. (2.12), we take the m_W data at 95% Confidence Level (C.L.) with the χ^2 profile-likelihood fit,

$$\chi^2 = \frac{(m_W^{\rm 2HDM} - m_W^{\rm obs})^2}{\sum \sigma_{m_W}^2}. \tag{3.1}$$

JHEP10(2022)048

After taking into account the experiment uncertainties, we have

$$\Delta m_W^{\rm 2HDM}|_{\rm ex} \in (36.3, 103.4)\ {\rm MeV}, \tag{3.2}$$

and if considering SM theoretical uncertainties as well, it is $\Delta m_W^{\rm 2HDM}|_{\rm th+ex} \in (31.1, 108.9)$ MeV for the 6 parameter scan at 95% C.L.. We will only take $\Delta m_W^{\rm 2HDM}|_{\rm ex}$ as condition of m_W for CDF-II in the following study.[3]

3.2 SFOEWPT under LHC measurements

As discussed above, after scanning the entire parameter space of Type-I and Type-II 2HDM, we obtain the sector which is allowed by current limits and also satisfies the SFOEWPT requirement.

As shown in figure 3, the grey points meet all the conditions of current various measurements (except for m_W at CDF-II) and SFOEWPT in both types. For Type-I and Type-II, favored mass region are different:

- Type-I: to satisfy SFOEWPT and current limits, m_H distributes in region $(125, 1000)$ GeV with $\tan\beta$ varying from 1 to 50. Mass splitting $m_{H^\pm} - m_H$ and $m_A - m_H$ distribute in region $(-400, 400)$ GeV.

- Type-II: compared to Type-I, Type-II is more limited due to the limited $\tan\beta$ region. m_H distributes in region $(125, 1000)$ GeV,[4] while $\tan\beta$ is limited in interval $(1, 12)$. Mass splitting $\Delta m_C = m_{H^\pm} - m_H$ varies in region $(-200, 300)$ GeV, while $\Delta m_A = m_A - m_H$ varies in region $(-200, -30)$ and $(30, 300)$ GeV.

In order to further illustrate the constraints of SFOEWPT on 2HDMs' parameter space, in appendix figure 4, we provide the allowed parameter space in the plane of $m_H - \tan\beta$ without SFOEWPT requirment. Together with figure 3, it is clear that SFOEWPT excludes the parameter space with $m_H < 1000$ GeV. To summarize, SFOEWPT requires the mass of non-SM Higgs $H/A/H^\pm$ to be smaller than 1 TeV for both types and a certain amount of splitting between them for Type-II 2HDM.[5] Comparing with the right panel of figure 2, it is clear that the uplifted m_W is consistent with SFOEWPT requirement.

3.3 SFOEWPT under Higgs, Z and W precision measurements

As discussed above, SFOEWPT, Higgs precision measurements at one-loop level, and Z-pole physics (oblique parameter S, T, U) are all connected by heavy Higgs mass splitting. In more detail, figure 2 and eq. (2.12) tells that non-zero $\Delta S/T$ is needed for uplifting m_W. But Higgs and Z-pole physics have strong constraints on the value of $\Delta S/T$. As presented in figure 3, the green points meets all these Higgs, Z-pole, m_W and SFOEWPT conditions.

[3] There is no apparent difference found for $\Delta m_W^{\rm 2HDM}|_{\rm ex}$ and $\Delta m_W^{\rm 2HDM}|_{\rm th+ex}$ in our study.

[4] As explained, we do not include flavor constraints since some channels can not explained by Type-II 2HDM. But if one wants to consider the constraint $m_{H^\pm} > 800$ GeV obtained from $\bar{B} \to X_s\gamma$ channel [95], the points with $m_H < 550$ GeV will be totally excluded.

[5] We also note that such non-degenerate mass spectrum in 2HDM can be explored directly at future 100 TeV hadron colliders [100, 101].

JHEP10(2022)048

Compared to the grey points, we can see the allowed $\tan\beta, m_H, \Delta m_A$ and Δm_C region of green points indicates that an apparent mass splitting is needed to raise the W-boson mass. Another feature is they mainly locate around the boundary region, which is mainly because current electroweak measurements is not precise enough, so the uplifted m_W in need can still be satisfied within 2HDM framework. As shown in our benchmark case figure 1, specific ΔT is in need. Since oblique parameters is type universal, thus Type-I and Type-II have similar features for green region.

However, future lepton colliders, such as CEPC, ILC, and FCC-ee, will measure electroweak parameters to unprecedented precision. As presented in table 1, uncertainties of oblique measurements in CEPC can be reduced to 1% level, which is one order smaller than current uncertainties. For the Higgs precision measurements, the works [54, 88, 90] have discussed them for the case of 2HDM systematically. Provided that there is no apparent deviation of Higgs and Z-pole properties from the SM predictions observed, or in other words, the future measurements turn out to be consistent with SM prediction, we take CEPC precision measurements as an example to study the impact from future lepton colliders. Finally as shown in figure 3, the red points represent spectrum meeting conditions of Higgs, Z-pole measurements, and SFOEWPT. We can see, the red region is strongly restricted to $\Delta m_C = 0$ or $\Delta m_C = \Delta m_A$ and vanishing Δm_A is strongly disfavored for both types. For Type-I, it is $\Delta m_C = \Delta m_A$ for $|\Delta m_A| \in (150, 350)$GeV, or $\Delta m_C = 0$ for $|\Delta m_A| \in (150, 350)$GeV. While for Type-II, it is $\Delta m_C = \Delta m_A$ and $\Delta m_A \in (150, 250)$GeV, and a point with $\Delta m_C = 0$ and $\Delta m_A = 150$GeV is also found. In both types, the red region and green region are separate from each other, which means Higgs+Z-pole measurements at CEPC can exclude the region for m_W at CDF-II.

On the other hand, if SFOEWPT with uplifted m_W in 2HDM is the true BSM scenario, deviations from SM prediction will be observed at future measurements with high confidence level.

4 Conclusion

In this work, we revisited the existence of a strong first order electroweak phase transition (SFOEWPT) in the Type-I and Type-II 2HDMs as the grey points in figure 3. At the same time, the latest precision measurement of the m_W at CDF-II, indicates possible existence of new particles with mass around electroweak scale. We studied them all in the framework of 2HDM.

In detail, we carried out a global analysis, including W boson mass m_W, SFOEWPT requirements, direct searches of scalar resonances at the LHC, and current LHC and future Higgs and Z-pole precision measurements at lepton colliders such as CEPC, ILC, FCC-ee. We found that,

1. Since in the 2HDM, $\Delta m_W^{\rm 2HDM}$ is directly related to oblique parameters as discussed, which is dependent on the heavy Higgs mass splitting of $\Delta m_A = m_A - m_H$ and $\Delta m_C = m_{H^\pm} - m_H$, we can see $\Delta m_W^{\rm 2HDM}$ is sensitive to heavy Higgs mass splitting. As a result, all these precision measurements and SFOEWPT in 2HDM are sensitive to non-SM Higgs mass splitting in 2HDM.

JHEP10(2022)048

2. Under current constraints, both Type-I and Type-II 2HDM can explain the SFOEWPT, Z-pole, Higgs precision measurements and m_W precision measurement of CDF-II at same time. In the figure 3, we have the green points satisfying all of them, under current various constraints. Generally the allowed region are

$$m_H \in (125, 950)\ \text{GeV}\,, \Delta m_{A/C} \in (-400, 400)\ \text{GeV}, \tan\beta \in (1, 50)$$

for Type-I, and they are divided into two regions $\Delta m_C > \Delta m_A$ when $\Delta m_C > 0$ and $\Delta m_C < \Delta m_A$ when $\Delta m_C < 0$, and only $\Delta m_A = 0$ is possibly allowed,

$$m_H \in (125, 900)\ \text{GeV}\,, \Delta m_{A/C} \in (-200, 300)\ \text{GeV}, \tan\beta \in (1, 10)$$

for Type-II. Similarly they are divided into two regions $\Delta m_C > \Delta m_A$ when $\Delta m_C > 0$ and $\Delta m_C < \Delta m_A$ when $\Delta m_C < 0$, but both $\Delta m_{A/C}$ can not reach 0.

3. With future precision measurements at CEPC, ILC, or FCC-ee, if there is no deviation to SM observed at Higgs or Z-pole physics, SFOEWPT is still allowed, but m_W from CDF-II can not be explained anymore by 2HDM. In other words, if 2HDM is the true BSM scenario after the run of lepton colliders, deviations from the SM prediction will be observed at future measurements with high confidence level.

   Such a constrained parameter space points out a clear direction for experimental studies and also for theoretical explorations for explaining other phenomenology, such as shrunk region of non-SM triple Higgs couplings involving the mass splittings.

Acknowledgments

We thank Jin Min Yang, Shufang Su, Yang Zhang for useful discussions and comments. M.Z. was supported by the National Natural Science Foundation of China (NNSFC) under Grant No. 12105118 and 11947118. H.S. is supported by the International Postdoctoral Exchange Fellowship Program. W.S. is supported by KIAS Individual Grant (PG084201) at Korea Institute for Advanced Study, and by the Junior Foundation of Sun Yat-sen University.

A Result under LHC Run-II

Here we have the initial scan results for both Type-I and Type-II, showing in the figure 4. These scan results only meet all theoretical constraints, current experimental constraints from LHC, different from the gray points of figure 3 which also considers conditions of SFOEWPT .

JHEP10(2022)048

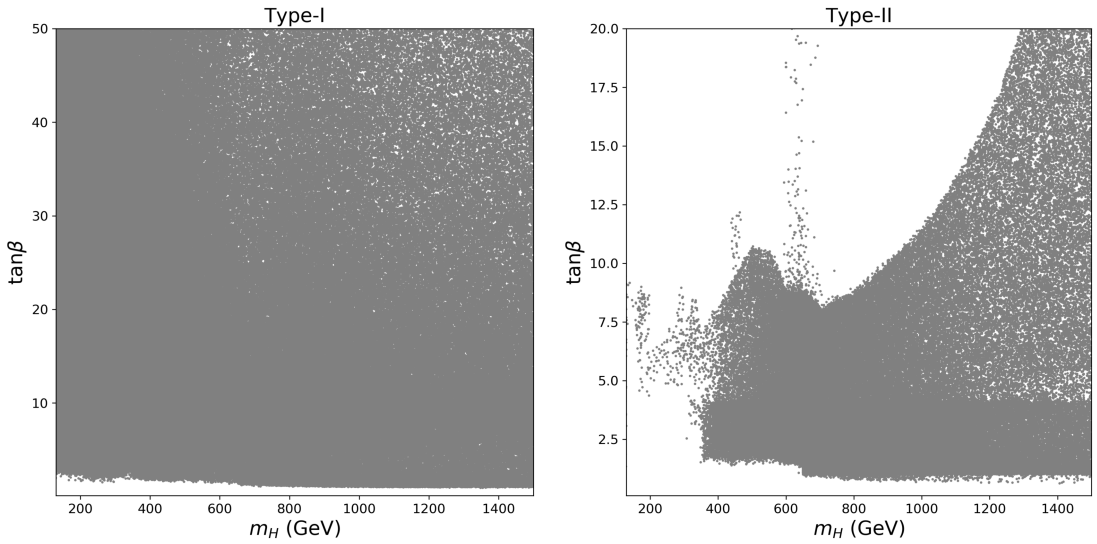

Figure 4. The allowed parameter space in the plane of $m_H - \tan\beta$ for Type-I (left) and Type-II (right) respectively. The grey points survive all theoretical constraints, current experimental constraints.

References

[1] ATLAS collaboration, *Observation of a new particle in the search for the Standard Model Higgs boson with the ATLAS detector at the LHC*, *Phys. Lett. B* **716** (2012) 1 [arXiv:1207.7214] [INSPIRE].

[2] CMS collaboration, *Observation of a New Boson at a Mass of 125 GeV with the CMS Experiment at the LHC*, *Phys. Lett. B* **716** (2012) 30 [arXiv:1207.7235] [INSPIRE].

[3] CDF collaboration, *High-precision measurement of the W boson mass with the CDF II detector*, *Science* **376** (2022) 170 [INSPIRE].

[4] Y.-Z. Fan, T.-P. Tang, Y.-L.S. Tsai and L. Wu, *Inert Higgs Dark Matter for CDF II W-Boson Mass and Detection Prospects*, *Phys. Rev. Lett.* **129** (2022) 091802 [arXiv:2204.03693] [INSPIRE].

[5] C.-T. Lu, L. Wu, Y. Wu and B. Zhu, *Electroweak precision fit and new physics in light of the <math display="inline"><mi>W</mi></math> boson mass*, *Phys. Rev. D* **106** (2022) 035034 [arXiv:2204.03796] [INSPIRE].

[6] P. Athron, A. Fowlie, C.-T. Lu, L. Wu, Y. Wu and B. Zhu, *The W boson Mass and Muon $g-2$: Hadronic Uncertainties or New Physics?*, arXiv:2204.03996 [INSPIRE].

[7] G.-W. Yuan, L. Zu, L. Feng, Y.-F. Cai and Y.-Z. Fan, *Hint on new physics from the W-boson mass excess—axion-like particle, dark photon or Chameleon dark energy*, arXiv:2204.04183 [INSPIRE].

[8] A. Strumia, *Interpreting electroweak precision data including the W-mass CDF anomaly*, *JHEP* **08** (2022) 248 [arXiv:2204.04191] [INSPIRE].

[9] J.M. Yang and Y. Zhang, *Low energy SUSY confronted with new measurements of W-boson mass and muon g-2*, *Sci. Bull.* **67** (2022) 1430 [arXiv:2204.04202] [INSPIRE].

JHEP10(2022)048

[10] J. de Blas, M. Pierini, L. Reina and L. Silvestrini, *Impact of the recent measurements of the top-quark and W-boson masses on electroweak precision fits*, arXiv:2204.04204 [INSPIRE].

[11] C.-R. Zhu, M.-Y. Cui, Z.-Q. Xia, Z.-H. Yu, X. Huang, Q. Yuan et al., *GeV antiproton/gamma-ray excesses and the W-boson mass anomaly: three faces of* $\sim 60-70$ *GeV dark matter particle?*, arXiv:2204.03767 [INSPIRE].

[12] J.M. Cline, *Baryogenesis*, in *Les Houches Summer School - Session 86: Particle Physics and Cosmology: The Fabric of Spacetime*, 9, 2006 [hep-ph/0609145] [INSPIRE].

[13] D.E. Morrissey and M.J. Ramsey-Musolf, *Electroweak baryogenesis*, *New J. Phys.* **14** (2012) 125003 [arXiv:1206.2942] [INSPIRE].

[14] N.S. Manton, *Topology in the Weinberg-Salam Theory*, *Phys. Rev. D* **28** (1983) 2019 [INSPIRE].

[15] F.R. Klinkhamer and N.S. Manton, *A Saddle Point Solution in the Weinberg-Salam Theory*, *Phys. Rev. D* **30** (1984) 2212 [INSPIRE].

[16] V.A. Kuzmin, V.A. Rubakov and M.E. Shaposhnikov, *On the Anomalous Electroweak Baryon Number Nonconservation in the Early Universe*, *Phys. Lett. B* **155** (1985) 36 [INSPIRE].

[17] K. Kajantie, M. Laine, K. Rummukainen and M.E. Shaposhnikov, *Is there a hot electroweak phase transition at* $m_H \gtrsim m_W$*?*, *Phys. Rev. Lett.* **77** (1996) 2887 [hep-ph/9605288] [INSPIRE].

[18] F. Csikor, Z. Fodor and J. Heitger, *Endpoint of the hot electroweak phase transition*, *Phys. Rev. Lett.* **82** (1999) 21 [hep-ph/9809291] [INSPIRE].

[19] M. Carena, Z. Liu and M. Riembau, *Probing the electroweak phase transition via enhanced di-Higgs boson production*, *Phys. Rev. D* **97** (2018) 095032 [arXiv:1801.00794] [INSPIRE].

[20] J.M. Cline and K. Kainulainen, *Electroweak baryogenesis and dark matter from a singlet Higgs*, *JCAP* **01** (2013) 012 [arXiv:1210.4196] [INSPIRE].

[21] J.M. Cline, K. Kainulainen and D. Tucker-Smith, *Electroweak baryogenesis from a dark sector*, *Phys. Rev. D* **95** (2017) 115006 [arXiv:1702.08909] [INSPIRE].

[22] M. Carena, M. Quirós and Y. Zhang, *Electroweak Baryogenesis from Dark-Sector CP-violation*, *Phys. Rev. Lett.* **122** (2019) 201802 [arXiv:1811.09719] [INSPIRE].

[23] J.M. Cline, G. Laporte, H. Yamashita and S. Kraml, *Electroweak Phase Transition and LHC Signatures in the Singlet Majoron Model*, *JHEP* **07** (2009) 040 [arXiv:0905.2559] [INSPIRE].

[24] G.D. Moore, *Measuring the broken phase sphaleron rate nonperturbatively*, *Phys. Rev. D* **59** (1999) 014503 [hep-ph/9805264] [INSPIRE].

[25] S.R. Coleman and E.J. Weinberg, *Radiative Corrections as the Origin of Spontaneous Symmetry Breaking*, *Phys. Rev. D* **7** (1973) 1888 [INSPIRE].

[26] P.B. Arnold and O. Espinosa, *The Effective potential and first order phase transitions: Beyond leading-order*, *Phys. Rev. D* **47** (1993) 3546 [*Erratum ibid.* **50** (1994) 6662] [hep-ph/9212235] [INSPIRE].

[27] W. Su, A.G. Williams and M. Zhang, *Strong first order electroweak phase transition in 2HDM confronting future Z & Higgs factories*, *JHEP* **04** (2021) 219 [arXiv:2011.04540] [INSPIRE].

JHEP10(2022)048

[28] N.K. Nielsen, *On the Gauge Dependence of Spontaneous Symmetry Breaking in Gauge Theories*, *Nucl. Phys. B* **101** (1975) 173 [INSPIRE].

[29] K. Kainulainen, V. Keus, L. Niemi, K. Rummukainen, T.V.I. Tenkanen and V. Vaskonen, *On the validity of perturbative studies of the electroweak phase transition in the Two Higgs Doublet model*, *JHEP* **06** (2019) 075 [arXiv:1904.01329] [INSPIRE].

[30] F.P. Huang and C.S. Li, *Electroweak baryogenesis in the framework of the effective field theory*, *Phys. Rev. D* **92** (2015) 075014 [arXiv:1507.08168] [INSPIRE].

[31] F.P. Huang, Z. Qian and M. Zhang, *Exploring dynamical CP-violation induced baryogenesis by gravitational waves and colliders*, *Phys. Rev. D* **98** (2018) 015014 [arXiv:1804.06813] [INSPIRE].

[32] R. Zhou and L. Bian, *Gravitational wave and electroweak baryogenesis with two Higgs doublet models*, *Phys. Lett. B* **829** (2022) 137105 [arXiv:2001.01237] [INSPIRE].

[33] J. Bernon, L. Bian and Y. Jiang, *A new insight into the phase transition in the early Universe with two Higgs doublets*, *JHEP* **05** (2018) 151 [arXiv:1712.08430] [INSPIRE].

[34] B. Barman, A. Dutta Banik and A. Paul, *Singlet-doublet fermionic dark matter and gravitational waves in a two-Higgs-doublet extension of the Standard Model*, *Phys. Rev. D* **101** (2020) 055028 [arXiv:1912.12899] [INSPIRE].

[35] D. Croon, O. Gould, P. Schicho, T.V.I. Tenkanen and G. White, *Theoretical uncertainties for cosmological first-order phase transitions*, *JHEP* **04** (2021) 055 [arXiv:2009.10080] [INSPIRE].

[36] P. Schicho, T.V.I. Tenkanen and G. White, *Combining thermal resummation and gauge invariance for electroweak phase transition*, arXiv:2203.04284 [INSPIRE].

[37] P.M. Schicho, T.V.I. Tenkanen and J. Österman, *Robust approach to thermal resummation: Standard Model meets a singlet*, *JHEP* **06** (2021) 130 [arXiv:2102.11145] [INSPIRE].

[38] L. Niemi, P. Schicho and T.V.I. Tenkanen, *Singlet-assisted electroweak phase transition at two loops*, *Phys. Rev. D* **103** (2021) 115035 [arXiv:2103.07467] [INSPIRE].

[39] P. Basler, M. Krause, M. Muhlleitner, J. Wittbrodt and A. Wlotzka, *Strong First Order Electroweak Phase Transition in the CP-Conserving 2HDM Revisited*, *JHEP* **02** (2017) 121 [arXiv:1612.04086] [INSPIRE].

[40] P. Basler, M. Mühlleitner and J. Wittbrodt, *The CP-Violating 2HDM in Light of a Strong First Order Electroweak Phase Transition and Implications for Higgs Pair Production*, *JHEP* **03** (2018) 061 [arXiv:1711.04097] [INSPIRE].

[41] P. Basler, M. Mühlleitner and J. Müller, *Electroweak Phase Transition in Non-Minimal Higgs Sectors*, *JHEP* **05** (2020) 016 [arXiv:1912.10477] [INSPIRE].

[42] D. López-Val and T. Robens, Δr *and the W-boson mass in the singlet extension of the standard model*, *Phys. Rev. D* **90** (2014) 114018 [arXiv:1406.1043] [INSPIRE].

[43] T.D. Lee, *A Theory of Spontaneous T Violation*, *Phys. Rev. D* **8** (1973) 1226 [INSPIRE].

[44] G.C. Branco, P.M. Ferreira, L. Lavoura, M.N. Rebelo, M. Sher and J.P. Silva, *Theory and phenomenology of two-Higgs-doublet models*, *Phys. Rept.* **516** (2012) 1 [arXiv:1106.0034] [INSPIRE].

[45] D. Lopez-Val and J. Solà, *Delta r in the Two-Higgs-Doublet Model at full one loop level – and beyond*, *Eur. Phys. J. C* **73** (2013) 2393 [arXiv:1211.0311] [INSPIRE].

JHEP10(2022)048

[46] P. Bambade et al., *The International Linear Collider: A Global Project*, arXiv:1903.01629 [INSPIRE].

[47] FCC collaboration, *FCC Physics Opportunities*: Future Circular Collider Conceptual Design Report Volume 1, *Eur. Phys. J. C* **79** (2019) 474 [INSPIRE].

[48] FCC collaboration, *FCC-ee: The Lepton Collider*: Future Circular Collider Conceptual Design Report Volume 2, *Eur. Phys. J. ST* **228** (2019) 261 [INSPIRE].

[49] CEPC Study Group collaboration, *CEPC Conceptual Design Report: Volume 2 - Physics & Detector*, arXiv:1811.10545 [INSPIRE].

[50] CEPC Physics-Detector Study Group collaboration, *The CEPC input for the European Strategy for Particle Physics - Physics and Detector*, arXiv:1901.03170 [INSPIRE].

[51] L. Wang, J.M. Yang and Y. Zhang, *Two-Higgs-doublet models in light of current experiments: a brief review*, *Commun. Theor. Phys.* **74** (2022) 097202 [arXiv:2203.07244] [INSPIRE].

[52] J.F. Gunion and H.E. Haber, *The CP conserving two Higgs doublet model: The Approach to the decoupling limit*, *Phys. Rev. D* **67** (2003) 075019 [hep-ph/0207010] [INSPIRE].

[53] I.F. Ginzburg and I.P. Ivanov, *Tree-level unitarity constraints in the most general 2HDM*, *Phys. Rev. D* **72** (2005) 115010 [hep-ph/0508020] [INSPIRE].

[54] J. Gu, H. Li, Z. Liu, S. Su and W. Su, *Learning from Higgs Physics at Future Higgs Factories*, *JHEP* **12** (2017) 153 [arXiv:1709.06103] [INSPIRE].

[55] ALEPH, DELPHI, L3, OPAL, LEP collaborations, *Search for Charged Higgs bosons: Combined Results Using LEP Data*, *Eur. Phys. J. C* **73** (2013) 2463 [arXiv:1301.6065] [INSPIRE].

[56] ALEPH, DELPHI, L3, OPAL, LEP Working Group for Higgs Boson Searches collaborations, *Search for neutral MSSM Higgs bosons at LEP*, *Eur. Phys. J. C* **47** (2006) 547 [hep-ex/0602042] [INSPIRE].

[57] CMS collaboration, *Search for MSSM Higgs bosons decaying to $\mu + \mu -$ in proton-proton collisions at $\sqrt{s} = 13$ TeV*, *Phys. Lett. B* **798** (2019) 134992 [arXiv:1907.03152] [INSPIRE].

[58] ATLAS collaboration, *Search for scalar resonances decaying into $\mu^+\mu^-$ in events with and without b-tagged jets produced in proton-proton collisions at $\sqrt{s} = 13$ TeV with the ATLAS detector*, *JHEP* **07** (2019) 117 [arXiv:1901.08144] [INSPIRE].

[59] CMS collaboration, *Search for beyond the standard model Higgs bosons decaying into a $\mathrm{b\bar{b}}$ pair in pp collisions at $\sqrt{s} = 13$ TeV*, *JHEP* **08** (2018) 113 [arXiv:1805.12191] [INSPIRE].

[60] ATLAS collaboration, *Search for heavy neutral Higgs bosons produced in association with b-quarks and decaying into b-quarks at $\sqrt{s} = 13$ TeV with the ATLAS detector*, *Phys. Rev. D* **102** (2020) 032004 [arXiv:1907.02749] [INSPIRE].

[61] CMS collaboration, *Search for additional neutral MSSM Higgs bosons in the $\tau\tau$ final state in proton-proton collisions at $\sqrt{s} = 13$ TeV*, *JHEP* **09** (2018) 007 [arXiv:1803.06553] [INSPIRE].

[62] CMS collaboration, *Search for a low-mass $\tau^+\tau^-$ resonance in association with a bottom quark in proton-proton collisions at $\sqrt{s} = 13$ TeV*, *JHEP* **05** (2019) 210 [arXiv:1903.10228] [INSPIRE].

JHEP10(2022)048

[63] ATLAS collaboration, *Search for heavy Higgs bosons decaying into two tau leptons with the ATLAS detector using pp collisions at $\sqrt{s} = 13$ TeV*, *Phys. Rev. Lett.* **125** (2020) 051801 [arXiv:2002.12223] [INSPIRE].

[64] CMS collaboration, *Search for a standard model-like Higgs boson in the mass range between 70 and 110 GeV in the diphoton final state in proton-proton collisions at $\sqrt{s} = 8$ and 13 TeV*, *Phys. Lett. B* **793** (2019) 320 [arXiv:1811.08459] [INSPIRE].

[65] CMS collaboration, *Search for physics beyond the standard model in high-mass diphoton events from proton-proton collisions at $\sqrt{s} = 13$ TeV*, *Phys. Rev. D* **98** (2018) 092001 [arXiv:1809.00327] [INSPIRE].

[66] ATLAS collaboration, *Search for Scalar Diphoton Resonances in the Mass Range $65 - 600$ GeV with the ATLAS Detector in pp Collision Data at $\sqrt{s} = 8$ TeV*, *Phys. Rev. Lett.* **113** (2014) 171801 [arXiv:1407.6583] [INSPIRE].

[67] ATLAS collaboration, *Search for new phenomena in high-mass diphoton final states using 37 fb^{-1} of proton–proton collisions collected at $\sqrt{s} = 13$ TeV with the ATLAS detector*, *Phys. Lett. B* **775** (2017) 105 [arXiv:1707.04147] [INSPIRE].

[68] ATLAS collaboration, *Search for resonances in the 65 to 110 GeV diphoton invariant mass range using 80 fb^{-1} of pp collisions collected at $\sqrt{s} = 13$ TeV with the ATLAS detector*, Tech. Rep. ATLAS-CONF-2018-025, CERN, Geneva, Switzerland (2018).

[69] CMS collaboration, *Search for heavy Higgs bosons decaying to a top quark pair in proton-proton collisions at $\sqrt{s} = 13$ TeV*, *JHEP* **04** (2020) 171 [arXiv:1908.01115] [INSPIRE].

[70] CMS collaboration, *Search for a new scalar resonance decaying to a pair of Z bosons in proton-proton collisions at $\sqrt{s} = 13$ TeV*, *JHEP* **06** (2018) 127 [*Erratum ibid.* **03** (2019) 128] [arXiv:1804.01939] [INSPIRE].

[71] ATLAS collaboration, *Search for heavy ZZ resonances in the $\ell^+\ell^-\ell^+\ell^-$ and $\ell^+\ell^-\nu\bar{\nu}$ final states using proton–proton collisions at $\sqrt{s} = 13$ TeV with the ATLAS detector*, *Eur. Phys. J. C* **78** (2018) 293 [arXiv:1712.06386] [INSPIRE].

[72] CMS collaboration, *Search for a heavy Higgs boson decaying to a pair of W bosons in proton-proton collisions at $\sqrt{s} = 13$ TeV*, *JHEP* **03** (2020) 034 [arXiv:1912.01594] [INSPIRE].

[73] ATLAS collaboration, *Search for heavy resonances decaying into WW in the $e\nu\mu\nu$ final state in pp collisions at $\sqrt{s} = 13$ TeV with the ATLAS detector*, *Eur. Phys. J. C* **78** (2018) 24 [arXiv:1710.01123] [INSPIRE].

[74] CMS collaboration, *Search for a pseudoscalar boson decaying into a Z boson and the 125 GeV Higgs boson in $\ell^+\ell^- b\bar{b}$ final states*, *Phys. Lett. B* **748** (2015) 221 [arXiv:1504.04710] [INSPIRE].

[75] CMS collaboration, *Search for a heavy pseudoscalar boson decaying to a Z and a Higgs boson at $\sqrt{s} = 13$ TeV*, *Eur. Phys. J. C* **79** (2019) 564 [arXiv:1903.00941] [INSPIRE].

[76] ATLAS collaboration, *Search for a CP-odd Higgs boson decaying to Zh in pp collisions at $\sqrt{s} = 8$ TeV with the ATLAS detector*, *Phys. Lett. B* **744** (2015) 163 [arXiv:1502.04478] [INSPIRE].

JHEP10(2022)048

[77] ATLAS collaboration, *Search for heavy resonances decaying into a W or Z boson and a Higgs boson in final states with leptons and b-jets in 36 fb^{-1} of $\sqrt{s} = 13$ TeV pp collisions with the ATLAS detector*, *JHEP* **03** (2018) 174 [*Erratum ibid.* **11** (2018) 051] [arXiv:1712.06518] [INSPIRE].

[78] CMS collaboration, *Searches for a heavy scalar boson H decaying to a pair of 125 GeV Higgs bosons hh or for a heavy pseudoscalar boson A decaying to Zh, in the final states with $h \to \tau\tau$*, *Phys. Lett. B* **755** (2016) 217 [arXiv:1510.01181] [INSPIRE].

[79] CMS collaboration, *Search for a heavy pseudoscalar Higgs boson decaying into a 125 GeV Higgs boson and a Z boson in final states with two tau and two light leptons at $\sqrt{s} = 13$ TeV*, *JHEP* **03** (2020) 065 [arXiv:1910.11634] [INSPIRE].

[80] CMS collaboration, *Search for Higgs boson pair production in the $bb\tau\tau$ final state in proton-proton collisions at $\sqrt(s) = 8$ TeV*, *Phys. Rev. D* **96** (2017) 072004 [arXiv:1707.00350] [INSPIRE].

[81] CMS collaboration, *Combination of searches for Higgs boson pair production in proton-proton collisions at $\sqrt{s} = 13$ TeV*, *Phys. Rev. Lett.* **122** (2019) 121803 [arXiv:1811.09689] [INSPIRE].

[82] ATLAS collaboration, *Searches for Higgs boson pair production in the $hh \to bb\tau\tau, \gamma\gamma WW^*, \gamma\gamma bb, bbbb$ channels with the ATLAS detector*, *Phys. Rev. D* **92** (2015) 092004 [arXiv:1509.04670] [INSPIRE].

[83] ATLAS collaboration, *Combination of searches for Higgs boson pairs in pp collisions at $\sqrt{s} = 13$ TeV with the ATLAS detector*, *Phys. Lett. B* **800** (2020) 135103 [arXiv:1906.02025] [INSPIRE].

[84] ATLAS collaboration, *Search for a heavy Higgs boson decaying into a Z boson and another heavy Higgs boson in the $\ell\ell bb$ final state in pp collisions at $\sqrt{s} = 13$ TeV with the ATLAS detector*, *Phys. Lett. B* **783** (2018) 392 [arXiv:1804.01126] [INSPIRE].

[85] CMS collaboration, *Search for new neutral Higgs bosons through the $H \to ZA \to \ell^+\ell^-\mathrm{b\bar{b}}$ process in pp collisions at $\sqrt{s} = 13$ TeV*, *JHEP* **03** (2020) 055 [arXiv:1911.03781] [INSPIRE].

[86] F. Kling, S. Su and W. Su, *2HDM Neutral Scalars under the LHC*, *JHEP* **06** (2020) 163 [arXiv:2004.04172] [INSPIRE].

[87] ALEPH, DELPHI, L3, OPAL, SLD, LEP Electroweak Working Group, SLD Electroweak Group, SLD Heavy Flavour Group collaborations, *Precision electroweak measurements on the Z resonance*, *Phys. Rept.* **427** (2006) 257 [hep-ex/0509008] [INSPIRE].

[88] N. Chen, T. Han, S. Su, W. Su and Y. Wu, *Type-II 2HDM under the Precision Measurements at the Z-pole and a Higgs Factory*, *JHEP* **03** (2019) 023 [arXiv:1808.02037] [INSPIRE].

[89] T. Han, S. Li, S. Su, W. Su and Y. Wu, *Comparative Studies of 2HDMs under the Higgs Boson Precision Measurements*, *JHEP* **01** (2021) 045 [arXiv:2008.05492] [INSPIRE].

[90] N. Chen, T. Han, S. Li, S. Su, W. Su and Y. Wu, *Type-I 2HDM under the Higgs and Electroweak Precision Measurements*, *JHEP* **08** (2020) 131 [arXiv:1912.01431] [INSPIRE].

[91] A. Sirlin and A. Ferroglia, *Radiative Corrections in Precision Electroweak Physics: a Historical Perspective*, *Rev. Mod. Phys.* **85** (2013) 263 [arXiv:1210.5296] [INSPIRE].

JHEP10(2022)048

[92] Particle Data Group collaboration, *Review of Particle Physics*, *PTEP* **2022** (2022) 083C01 [INSPIRE].

[93] ATLAS collaboration, *Combination of searches for non-resonant and resonant Higgs boson pair production in the $b\bar{b}\gamma\gamma$, $b\bar{b}\tau^+\tau^-$ and $b\bar{b}b\bar{b}$ decay channels using pp collisions at $\sqrt{s} = 13$ TeV with the ATLAS detector*, Tech. Rep. ATLAS-CONF-2021-052, CERN, Geneva, Switzerland (2021).

[94] O. Atkinson, M. Black, A. Lenz, A. Rusov and J. Wynne, *Cornering the Two Higgs Doublet Model Type II*, *JHEP* **04** (2022) 172 [arXiv:2107.05650] [INSPIRE].

[95] M. Misiak, A. Rehman and M. Steinhauser, *Towards $\overline{B} \to X_s\gamma$ at the NNLO in QCD without interpolation in m_c*, *JHEP* **06** (2020) 175 [arXiv:2002.01548] [INSPIRE].

[96] M. Misiak and M. Steinhauser, *Weak radiative decays of the B meson and bounds on $M_{H^\pm}$ in the Two-Higgs-Doublet Model*, *Eur. Phys. J. C* **77** (2017) 201 [arXiv:1702.04571] [INSPIRE].

[97] A. Arbey, F. Mahmoudi, O. Stal and T. Stefaniak, *Status of the Charged Higgs Boson in Two Higgs Doublet Models*, *Eur. Phys. J. C* **78** (2018) 182 [arXiv:1706.07414] [INSPIRE].

[98] BaBar collaboration, *Evidence for an excess of $\bar{B} \to D^{(*)}\tau^-\bar{\nu}_\tau$ decays*, *Phys. Rev. Lett.* **109** (2012) 101802 [arXiv:1205.5442] [INSPIRE].

[99] P. Basler and M. Mühlleitner, *BSMPT (Beyond the Standard Model Phase Transitions): A tool for the electroweak phase transition in extended Higgs sectors*, *Comput. Phys. Commun.* **237** (2019) 62 [arXiv:1803.02846] [INSPIRE].

[100] F. Kling, H. Li, A. Pyarelal, H. Song and S. Su, *Exotic Higgs Decays in Type-II 2HDMs at the LHC and Future 100 TeV Hadron Colliders*, *JHEP* **06** (2019) 031 [arXiv:1812.01633] [INSPIRE].

[101] S. Li, H. Song and S. Su, *Probing Exotic Charged Higgs Decays in the Type-II 2HDM through Top Rich Signal at a Future 100 TeV pp Collider*, *JHEP* **11** (2020) 105 [arXiv:2005.00576] [INSPIRE].

JHEP10(2022)048